

30  
6/17/89 J.S. (3)

CONF-890335-1601  
SLAC-PUB-4905  
March 1989  
(A)

BUNCH LENGTHENING CALCULATIONS FOR THE SLC DAMPING RINGS\*

KARL L. F. BANE AND RONALD D. RUTH

Stanford Linear Accelerator Center, Stanford University, Stanford, California 94309

SLAC-PUB--4905

DE89 012278

ABSTRACT

The problem of bunch lengthening in electron storage rings has been treated by many people, and there have been many experiments. In the typical experiment, the theory is used to determine the impedance of the ring. What has been lacking thus far, however, is a calculation of bunch lengthening that uses a carefully calculated ring impedance (or wakefield).

In this paper we begin by finding the potential well distortion due to some very simple impedance models, in order to illustrate different types of bunch lengthening behavior. We then give a prescription for extending potential well calculations into the turbulent regime once the threshold is known. Then finally, using the wakefield calculated in Ref. 1 for the SLC damping rings, combined with the measured value of the threshold given in Ref. 2, we calculate bunch lengthening for the damping rings, and compare the results with the measurements.

1. POTENTIAL WELL DISTORTION

The self-consistent beam current distribution in an electron machine, below the turbulent threshold, is given by<sup>3</sup>

$$I(t) = K \exp \left( -\frac{t^2}{2\sigma_0^2} + \frac{1}{V_{r,f}\sigma_0^2} \int_0^t V_{ind}(t') dt' \right) \quad (1)$$

with  $\sigma_0$  the natural bunch length,  $V_{r,f}$  the slope of the rf voltage at the position of the bunch and  $V_{ind}$  the transient induced voltage. In our notation a smaller value of  $t$  signifies an earlier point in time, with  $t = 0$  the synchronous point for a low current beam. The induced voltage  $V_{ind}$  is given by

$$V_{ind}(t) = - \int_0^{\infty} W(t') I(t-t') dt' \quad (2)$$

with  $W(t)$  the longitudinal Green function wakefield. The value of the normalization constant  $K$  in Eq. (1) is such that the complete integral of  $I(t)$  is equal to the total charge in the bunch  $Q$ . If we know the Green function wakefield then Eq. (1) can be solved numerically to give the current distribution of the bunch in the presence of wakefields. Since  $V_{ind}$  at time  $t$  depends only on the current at more negative (earlier) times, the solution of Eq. (1) is straightforward if we begin at the head of the bunch (where  $V_{ind} = 0$ ) and proceed toward the tail. Taking the derivative of both sides of Eq. (1) yields an alternative form of it:

$$\frac{\dot{I}}{I} = -\frac{t}{\sigma_0^2} + \frac{V_{ind}}{V_{r,f}\sigma_0^2} \quad (3)$$

In what follows, all distances will be given in terms of  $\sigma_0$ . Thus the independent variable becomes  $x = t/\sigma_0$ . Of particular interest will be the rms length  $\sigma_x$ , the full-width-at-half-maximum  $x_{FWHM}$ , and the centroid shift ( $\bar{x}$ ) of the current distribution. The ratio of the first two quantities is a measure of the similarity of the distribution to a Gaussian. Due to energy conservation, the third quantity, when multiplied by  $-V_{r,f}\sigma_0$ , gives the higher mode losses.

2. SOME SIMPLE IMPEDANCE MODELS

Over a frequency interval, the impedance of vacuum chamber elements can often be characterized by a simple electrical circuit element—an inductor, a resistor, or a capacitor. In this section we study the potential well distortion when the whole ring can be characterized by these simple models.

\*Work supported by the Department of Energy, contract DE-AC03-76SF00515.

2.1 An Inductive Impedance

The SLC damping ring impedance is dominated by objects—such as shallow transitions, shallow cavities, bellows, or bumps in the vacuum chamber—that can be modelled by an inductor over a range of bunch lengths.<sup>4</sup> For a purely inductive object the induced voltage is given by  $V_{ind} = -L di/dt$ , with the constant  $L$  the inductance. We note that this model is non-physical in that it is lossless. Although a solution of the potential well problem for an inductive impedance is given in Ref. 3, we present it here again in order to complete our picture of bunch lengthening in storage rings.

For a purely inductive impedance, Eq. (3) can be written as

$$y' = -\frac{xy}{1+y} \quad (4)$$

with prime denoting the derivative with respect to  $x = t/\sigma_0$ . The normalized current is given by  $y = LI/(V\sigma_0^2)$ ; the normalized charge  $\Gamma$  (the complete integral of  $y$ ) equals  $LQ/(V\sigma_0^2)$ . The normalized induced voltage  $v_{ind} \equiv V_{ind}/(V_{r,f}\sigma_0) = -y'$ .

The numerical solution of Eq. (4), for several values of  $\Gamma$ , is shown in Fig. 1(a). Note that the charge distribution for a perfect inductor is symmetric about  $x = 0$  (since there are no losses) and is more bulbous than a Gaussian distribution. From Eq. (4) it is apparent that the solution is parabolic whenever  $y \gg 1$ . In Fig. 1(b) we display  $\sigma_x$  and  $x_{FWHM}/2.355$  (the dashes) as functions of  $\Gamma$ . For large currents  $\sigma_x$  varies roughly as  $\Gamma^{1/3}$ .

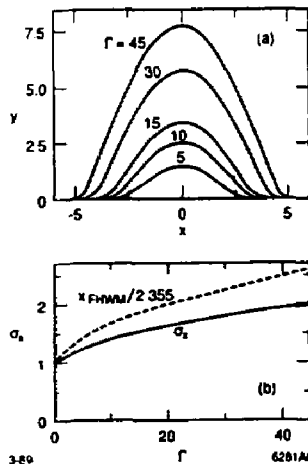


Fig. 1. An inductive impedance: (a) the bunch shape for several values of bunch population, and (b) the bunch length variation as a function of current.

2.2 A Resistive Impedance

Deep cavities, such as the rf cavities of the damping rings, tend to be resistive or somewhat capacitive to a beam over the normal range of bunch lengths. For an ideal resistive object, the induced voltage can be written as  $V_{ind} = -IR$ , with the constant  $R$  the resistance. Note that an ideal resistor is also

DISTRIBUTION OF THIS DOCUMENT IS UNLIMITED

not physical: there must be a phase shift, even if slight, between the bunch current and the induced voltage of a vacuum chamber object. For a resistive impedance, Eq. (3) becomes

$$y' = -(x+y)y \quad (5)$$

with  $y = RI/(\dot{V}\sigma_0)$  and  $\Gamma = RQ/(\dot{V}\sigma_0^2)$ . Note that  $v_{ind} = -y$ .

Fig. 2(a) displays the solution to Eq. (5) for several values of  $\Gamma$ . As the current is increased the bunch tilts forward (up the rf wave) by an ever increasing amount, in order to compensate for the increased, higher mode losses. Fig. 2(b) shows  $\sigma_x$  and  $x_{FWHM}/2.355$  (the dashes). We see that the bunch length increases only very slowly in a resistive machine. The dots give the centroid shift ( $x$ ) of the bunch. It can be approximated by  $\langle x \rangle = -\Gamma/(2\sqrt{\pi})$ , which is the centroid shift, assuming that the bunch shape does not change with  $\Gamma$ . We note that Papiernik et al.<sup>4</sup> have solved the potential well problem for the impedance of a pillbox cavity, and have obtained very similar results.

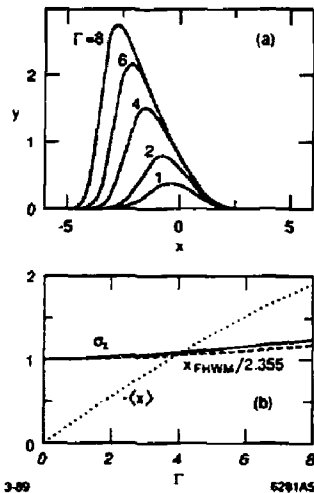


Fig. 2. A resistive impedance: (a) the bunch shape for several values of total charge and (b) the change of bunch length and centroid position (dots) with current.

### 2.3 A Capacitive Impedance

The wakefield of very short bunches in deep cavities is somewhat capacitive. For an ideal capacitive vacuum chamber object, the induced voltage is proportional to the integral of the current, with constant of proportionality  $-1/C$ , and  $C$  the capacitance. This model is unphysical in that it predicts that the energy loss of a bunch depends only on the total charge  $Q$ , and not on the peak current. For a purely capacitive impedance, Eq. (3) becomes

$$y' = -y \left[ x + \int_{-\infty}^x y(x') dx' \right] \quad (6)$$

with  $y = I/(\dot{V}_r C)$  and  $\Gamma = Q/(\dot{V}_r \sigma_0 C)$ . The solution to Eq. (6) closely approximates a Gaussian that has been shortened and shifted. Since the energy stored in a capacitor is  $Q^2/2C$ , the centroid shift is given by  $\langle x \rangle = -\Gamma/2$ . Figure 3 shows the bunch length dependence on  $\Gamma$ . By substituting a gaussian into Eq. (6), we can arrive at an analytical approximation of the bunch shortening, which for small current becomes  $\sigma_x \approx 1 - \Gamma/\sqrt{8\pi}$ . We note that bunch shortening has not been observed in storage rings, except at low currents in SPEAR, when the ring had many rf cavities.<sup>5</sup>

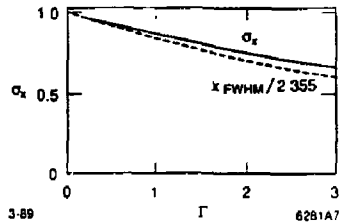


Fig. 3. Bunch shortening for a capacitive impedance.

## 3. THE INSTABILITY THRESHOLD

At some bunch population, there is an instability. The effect of this instability in an electron storage ring is to increase the energy spread of the equilibrium distribution. This is obviously a nonlinear process. As the bunch length increases, the bunch peak current decreases which decreases the longitudinal forces. Radiation damping then serves to reduce the bunch length. The competition between radiation damping and quantum excitation together with longitudinal instability leads to some equilibrium energy spread. The bunch length is related to this via the rf voltage plus potential well distortion.

Boussard<sup>6</sup> conjectured that the longitudinal instability in a bunched beam is due to a coasting-beam-like instability within the bunch. Qualitatively, the argument goes as follows: Consider an impedance which induces an instability which has a wavelength small compared to the bunch length. If the growth time of the instability is short compared to a synchrotron oscillation period, then the center of the bunch looks like a coasting beam except, of course, that it has a high peak current. Therefore, to estimate the threshold for instability one might use the coasting beam threshold<sup>7</sup> but replace  $I$  by  $I_{peak}$ .

The issue of the applicability of a coasting beam instability criterion to a bunched beam was studied in detail by J. M. Wang and C. Pellegrini.<sup>8</sup> They found that one obtains a coasting beam like instability condition provided that:

1. The impedance is broad band relative to the bunch spectrum (Fourier transform of the line density).
2. The growth rate is much greater than  $\omega_s$  (fast blowup).
3. The instability occurs at wavelengths much shorter than the bunch length.

Actually, the threshold which they obtain looks like the threshold for a coasting beam, but it has a different interpretation. It is a sufficient condition for no fast blowup. They also show that one obtains the usual type of coasting beam stability boundary except, of course, the boundary is for fast blowup.

The "threshold" condition for a Gaussian bunch is<sup>8</sup>

$$\frac{c^2 N |Z(\omega)/\omega|}{2\pi^{3/2} \sigma_r \sigma_z^2} \leq 1 \quad (7)$$

In Eq. (7), we have substituted the peak current for a Gaussian distribution. In this equation,  $\sigma_r$  must be interpreted as the actual bunch length. Since we have only a sufficient condition for fast instability, we only use Eq. (7) for scaling purposes. Unfortunately, we know of no reliable calculation of the precise threshold, although this should be possible using techniques in Ref. 8.

To proceed, we take the threshold from experimental data, and above the threshold we use Eq. (7) to scale the energy spread as

$$\sigma_r = \sigma_{r0} \left[ \frac{N}{N_{th}} \right]^{1/3} \quad (8)$$

Potential well bunch lengthening is then used to calculate the bunch form in a self-consistent manner.

#### 4. BUNCH LENGTHENING IN THE SLC DAMPING RINGS

The SLC damping rings have many changes in vacuum chamber cross-section. In an earlier paper<sup>1</sup> the longitudinal wakefields of the different vacuum chamber elements were computed for a short—1 mm—Gaussian bunch using T. Weiland's computer program TBCL.<sup>6</sup> All the individual contributions were then added up, giving a pseudo-Green function wake that represents the entire ring (see Fig. 4). By substituting this function into Eq. (1) we can calculate the current distribution up to the turbulent threshold current. Knowing  $N_{th}$  we can extend the calculation to higher currents if we replace  $\sigma_0$  by  $\sigma_0(N/N_{th})^{1/3}$  in Eq. (1).

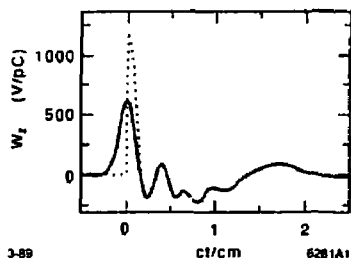


Fig. 4. The wakefield of a 1 mm Gaussian bunch in the SLC damping rings, and our Green function (dots).

We need to keep two things in mind when using our wakefield. First, since it represents the response to a 1 mm Gaussian bunch, it will be unable to resolve variations in bunch shape over distances that are short compared to 1 mm. But this limitation should not be a problem for our calculations because (i)  $c\sigma_0$  is large compared to 1 mm, (ii) the bunch becomes even longer at higher currents, and (iii) we expect the bunch forms to be smooth. Second, in order for us to use the wake as a Green function, the front of it needs to be modified so that it is zero for  $t < 0$ . We have evidence that the results (presented below) are not very sensitive to the details of this modification, provided that the changes are localized near  $t = 0$  and that the area under the curve remains unchanged. For our calculations, we have chosen to reflect the leading tail to the back, and then to add it to the existing wake (see the dotted curve of Fig. 4).

Figure 5 displays the bunch lengthening and centroid shift calculation results for the SLC damping rings when  $V_{rf} = 0.8$  MV. (The rf frequency is 714 MHz.) Length dimensions are again given in units of  $\sigma_0$  (at this rf voltage  $c\sigma_0 = 5$  mm). As for the inductive model, the distribution is more bulbous than a Gaussian. If we take the effective inductance of the ring to be 50 nH (see Ref. 1) we find that at  $N = 1.5 \times 10^{10}$   $\sigma_x = 1.33$  and  $x_{FWHM} = 3.69$  for the inductive model, which compare well with the values of, respectively, 1.38 and 3.93 found here. (To approximate the resistive behavior as well would require a more complicated model.) From Fig. 5(b) we see that there is a significant amount of higher mode losses.

Energy spread measurements performed on the North damping ring found that  $N_{th} \approx 1.5 \times 10^{10}$  at  $V_{rf} = 0.8$  MV.<sup>2</sup> Taking this threshold value, the bunch lengthening calculations were extended into the turbulent regime (indicated by the dashes in Fig. 5). We see that at  $N = 3 \times 10^{10}$  the rms bunch length is increased by 70%. Very precise measurements of the bunch shape as function of current have also been performed at  $V_{rf} = 0.8$  MV, using the bunch compressor of the Ring-to-Linac (RTL) transfer line and a downstream digitizable video screen.<sup>3</sup> In addition, the synchronous phase dependence on current has been measured. The results of these measurements are indicated by the plotting symbols in Fig. 5.

Finally, in Fig. 6 we present the bunch shapes for bunch populations of  $N = 0.7, 1.2, 2.1$  and  $2.9 \times 10^{10}$ .

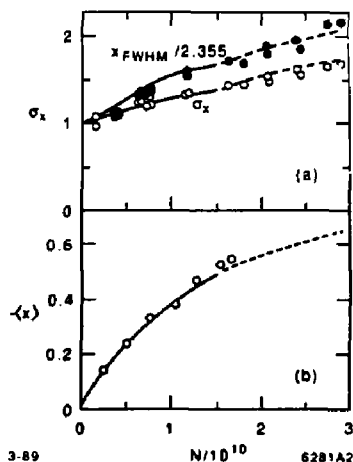


Fig. 5. (a) Bunch lengthening, and (b) the centroid shift calculated for the SLC damping rings at  $V_{rf} = 0.8$  MV. The symbols indicate the measurement results.

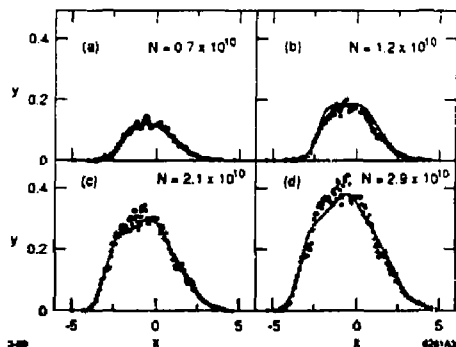


Fig. 6. The calculated damping ring bunch shapes for several current values, when  $V_{rf} = 0.8$  MV. Superimposed on the curves are measurement results.

The abscissas give  $x = t/\sigma_0$ , the ordinates are  $y = I Z_0 / (V \sigma_0)$  with  $Z_0 = 377 \Omega$ . Superimposed on the curves are the digitized measurement results. The fluctuations in the data (especially at the peaks) are due to nonuniformity in the response of the screen. Considering that there are no fit parameters, the agreement between the data and the calculations is quite good.

#### REFERENCES

1. K. L. F. Bane, SLAC-PUB-4618, (1988).
2. L. Rivkin et al, SLAC-PUB-4648, (1988).
3. J. Haissinski, *Il Nuovo Cimento* 18B, No. 1, 72 (1973).
4. A. Papiernik, M. Chatard-Moulin, B. Jecko, Proc. of the 9<sup>th</sup> Int. Conf. on High-Energy Acc., SLAC, 1974, p. 375.
5. P. B. Wilson et al, SLAC-PUB-1894, (1977).
6. D. Boussard, CERN LABII/RF/INT/75-2 (1975).
7. V. K. Neil and A. N. Sessler, *Rev. Sci. Instr.*, 36 429 (1965)
8. J. M. Wang and C. Pellegrini, Proc. of the 11<sup>th</sup> Int. Conf on High-Energy Accelerators, CERN, 1980, p. 554.
9. T. Weiland, DESY 82-015 (1982) and *Nucl. Inst. Meth.* 212, 13 (1983).

## **DISCLAIMER**

**This report was prepared as an account of work sponsored by an agency of the United States Government. Neither the United States Government nor any agency thereof, nor any of their employees, makes any warranty, express or implied, or assumes any legal liability or responsibility for the accuracy, completeness, or usefulness of any information, apparatus, product, or process disclosed, or represents that its use would not infringe privately owned rights. Reference herein to any specific commercial product, process, or service by trade name, trademark, manufacturer, or otherwise does not necessarily constitute or imply its endorsement, recommendation, or favoring by the United States Government or any agency thereof. The views and opinions of authors expressed herein do not necessarily state or reflect those of the United States Government or any agency thereof.**